Pre-treatment of automotive clear coat using atmospheric pressure plasma

A study of process parameters and their effect on surface energy and adhesion

by

SOFIA WILHELMSSON

Diploma work No. 113/2013
at Department of Materials and Manufacturing Technology
CHALMERS UNIVERSITY OF TECHNOLOGY
Gothenburg, Sweden

Diploma work in the Master programme Advanced Engineering Materials

Performed at:
Volvo Car Corporation
Dept. 93610
SE - 405 31 Gothenburg

Swerea IVF AB
Multi-material Design
SE - 431 22 Mölndal

Supervisor:
Peter Porsgaard, Technical Expert Polymer Applications
Volvo Car Corporation
SE- 405 31 Gothenburg

Examiner:
Prof. Mikael Rigdahl
Department of Materials and Manufacturing Technology
Chalmers University of Technology, SE - 412 96 Gothenburg

Pre-treatment of automotive clear coat using atmospheric pressure plasma
A study of process parameters and their effect on surface energy and adhesion
SOFIA WILHELMSSON

Diploma work no 113/2013
Department of Materials and Manufacturing Technology
Chalmers University of Technology
SE-412 96 Gothenburg
Sweden
Telephone + 46 (0)31-772 1000

Cover:
Photograph of a plasma plume created by the atmospheric pressure plasma equipment used in this project.

Reproservice
Gothenburg, Sweden 2013

Pre-treatment of automotive clear coat using atmospheric pressure plasma
A study of process parameters and their effect on surface energy and adhesion

SOFIA WILHELMSSON
Department of Materials and Manufacturing Technology
Chalmers University of Technology

SUMMARY

A study of the process parameters speed and working distance for an atmospheric pressure plasma equipment has been performed. This was done in order to investigate the possibility of using the equipment as pre-treatment for an automotive clear coat surface to enhance the surface energy and adhesion.

The effect of the equipment was measured by conducting contact angle measurements, surface energy calculation and lap shear testing. The study was conducted on non-contaminated "as received" substrate and on substrate purposely contaminated using the soil SebumTEFO. The effect of the atmospheric plasma treatment was also compared to a non-pre-treated and a solvent wiped surface.

The results from the experiments performed showed that increased surface energy and a higher adhesion are possible to accomplish using atmospheric plasma treatment. However the process parameter settings needed to obtain this effect differed between the non-contaminated and the contaminated surface.

Comparing the plasma treated samples with the solvent wiped and the non-pre-treated; the conclusion draw is that the plasma treated samples obtained higher adhesion, for non-contaminated and contaminated samples, respectively.

Keywords: surface pre-treatment, atmospheric pressure plasma, surface energy, adhesion

Acknowledgements

I would like to thank my examiner Prof. Mikael Rigdahl at Chalmers University of Technology for his valuable and constructive guidance.

I would like to express my great appreciation to my supervisor Peter Porsgaard at Volvo Car Corporation for his support and for initiating and giving me the opportunity to perform this thesis.

Special thanks should be given to Ola Albinsson and Åsa Lundevall at Swerea IVF for their enthusiastic help and guidance. I would also like to extend my thanks to all the staff at the Department of Process Development at Swerea IVF for their encouragement, interesting discussions, and assistance in the lab.

Furthermore I would like to thank my family and friends for the moral support during all my studies which have culminated in this thesis.

List of abbreviations and definitions

AR	As Received, material as it was delivered from supplier; in this project used to describe the status of a surface.
DOE	Design Of Experiments
PERU	Plasmabehandling för effektiv rutlimning (Plasma treatment for effective windshield bonding), a co-operation project between seven Swedish companies, established in order to investigate the effect of atmospheric pressure plasma treatment and its potential as a pre-treatment in the Swedish automotive industry.
RH	Relative Humidity
SebumTEFO	a commercial soil, originally developed by the Swedish textile research institute (Svenska Textilforskningsinstitutet TEFO); in this project also used to describe a status of a contaminated surface.
VCC	Volvo Car Corporation

Table of contents

1 Introduction

This chapter describes the problem this thesis aimed to mitigate and introduces the background of the project.

1.1 Background

Polymers are widely used in the automotive industry because of their low density and competitive price. Approximately 15-20 % of the total weight of a car is due to plastics [1] [2]. One field of application for polymers is as exterior components such as emblems and door mouldings. These components are often fastened by an adhesive or adhesive tape directly onto a painted car body, which also is a polymer surface. During transport and handling of the components, from manufacturing to assembly, there is a risk that the surfaces may be contaminated. A commonly used pre-treatment for cleaning the surface of the car body is solvent wiping using a paper cloth. Even though this pre-treatment is done, the adhesive bonds on the car body are often considered as a quality problem, some of them sooner or later experience failure. The solvent wiping itself is also a problem, causing a burden on both the production and on the environment [3]. It is also considered as an unreliable pre-treatment with low repeatability.

One general property of polymers is their low surface energy [4]. This makes the wettability poor, which could cause poor adhesion. A further problem when trying to form an adhesive bond is contamination on the surface. Therefore both cleaning and increase of the surface energy of the surface are highly important prior to forming an adhesive bond on a polymer surface.

Low pressure plasma has been used for surface treatment during the last decades [5]. The technique is however complicated and expensive to integrate in a production line, due to the batch-wise production in chambers and the high amounts of energy needed to create and maintain the low pressure [6].

Atmospheric pressure plasma treatment is a relatively new pre-treatment, rather unknown to the Swedish automotive industries. The equipment is connected to electricity and gas, but does not consume any chemicals or other material. Since there is no need for a special environment to create the plasma, this technique could be integrated in a continuous production line [3] [6]. Several studies have been conducted on the subject of the effect of atmospheric pressure plasma treatments on polymeric surfaces [7] [8] [9] [10] [11]. However, the equipment and gas used and the type of substrate differ, hence no general setting for process parameters exist.

Plasmabehandling för effektiv rutlimning (PERU) is a co-operation project between seven Swedish companies, established in order to investigate the effect of atmospheric pressure plasma treatment and its potential as a pre-treatment in the Swedish automotive industry [12]. This thesis project is a part of the PERU project, focused on the process parameters of the treatment, the effect on the surface energy and the adhesion strength of a painted substrate.

1.2 Purpose and aim

This project is conducted in co-operation with Volvo Car Corporation (VCC) and Swerea IVF. The purpose of this project is to contribute with information to the PERU project, regarding atmospheric pressure plasma treatment of a painted substrate supplied by VCC.

In more detail, the aim of this project is to study the effect of using an atmospheric pressure plasma set-up on the substrate, in terms of surface energy and adhesion strength. An untreated substrate and also a solvent wiped substrate are used as references. The treatment will be performed for both a substrate "as received" (AR) and for a purposefully contaminated substrate. Furthermore, the influence of the two parameters possible to alter, i.e. speed and working distance, for the atmospheric pressure plasma treatment will also be investigated.

2 Theory

In order to understand how adhesion and cleaning of surfaces work, this chapter will introduce the physical understanding of adhesion and wetting phenomena. This will be used in the experimental part as a basis for investigating the effect of the atmospheric pressure plasma treatment. A short introduction to pre-treatments including atmospheric pressure plasma is also included.

2.1 Adhesion and wetting

Adhesion could be described as; "the state in which two surfaces are held together by interfacial forces, which may consist of valence forces or interlocking action, or both." [13]. It is a complex topic and there is yet no single theory that explains the phenomenon.

The theories of adhesion are divided into two categories, mechanical adhesion and specific adhesion. The first category only includes the oldest theory, mechanical interlocking. The basic idea of the theory is that the adhesive fills the pores and the roughness of the surface and thereby mechanically locks the surfaces together. This is straightforward, but does not explain adhesion on a molecular level [14], or why it is possible to bond smooth surfaces [15]. One criticism against the theory is that the roughness of the surface simply contributes to a larger surface area, enabling more interaction of the specific adhesion type [14] [16].

The specific adhesion theories are of a physical and chemical nature. The most recent and widely used theory is thermodynamic adsorption [14] [15]. The essence of the theory is that if intimate contact (on molecular level) between the adhesive and the surface is accomplished, adhesion will occur due to forces at the interface. These forces are generally considered to be due to secondary bonds (physisorption), such as van der Waals forces. Some authors also include primary bonds (chemisorption), whereas some treat this as another theory called chemical or molecular adhesion/bonding [17]. Either way the intimate contact is needed since the range of the bonds is less than 5 Å [18]. Since no surfaces are that smooth, the adhesive must deform on the surface. This makes good wetting by the adhesive on the surface a criterion for good adhesion.

Wettability is "the ability of a solid surface to accept contact of and by a liquid, allowing it to spread freely and completely cover the surface." [13]. Wetting could be described as the balance of forces between the cohesion in a liquid and the adhesion between the surface and the liquid. The cohesion within the liquid creates a surface tension [N/m], equal to the surface energy [J/m²]. Wetting of a surface requires that the surface has a higher surface energy than the surface tension of the liquid. This is the driving force for treatments that increases the surface energy of surfaces prior bonding.

2.1.1 Contact angle and surface energy

The contact angle (θ) is the angle which a liquid resting on a surface forms towards the plane of the surface (Figure 2.1). It is a result of the tensions at the three interfaces solid-liquid, liquid-vapor and solid-vapor.

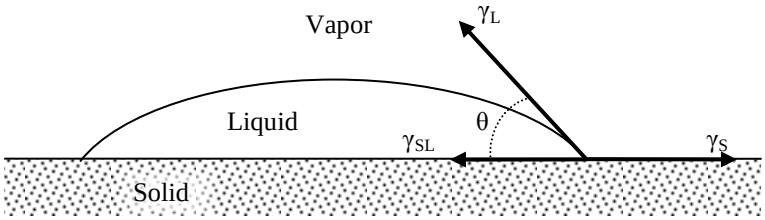

Figure 2.1: Drop on a flat surface showing the contact angle θ and the surface tensions.

Under the assumption of equilibrium, the relationship may be described by equation 2.1, known as Young's equation.

$$\gamma_L \cos\theta = \gamma_S - \gamma_{SL} \tag{2.1}$$

The surface energy (γ) is defined as the sum of the dispersions component (γ^d) and the polar component (γ^p), as seen in equation 2.2.

$$\gamma = \gamma^{\mathrm{d}} + \gamma^{\mathrm{p}} \tag{2.2}$$

The interfacial energy between the solid and the liquid, γ_{SL}, could be calculated using the harmonic mean theory proposed by Wu [19].

$$\gamma_{\mathrm{SL}} = \gamma_{\mathrm{S}} + \gamma_{\mathrm{L}} - 4\left[\frac{\gamma_{\mathrm{L}}^{\mathrm{d}}\gamma_{\mathrm{s}}^{\mathrm{d}}}{\gamma_{\mathrm{L}}^{\mathrm{d}} + \gamma_{\mathrm{s}}^{\mathrm{d}}} + \frac{\gamma_{\mathrm{L}}^{\mathrm{p}}\gamma_{\mathrm{s}}^{\mathrm{p}}}{\gamma_{\mathrm{L}}^{\mathrm{p}} + \gamma_{\mathrm{s}}^{\mathrm{p}}}\right] \tag{2.3}$$

Substituting equation 2.3 using equation 2.1, the following equation is provided:

$$\gamma_{\mathrm{L}}(1 + \cos\theta) = 4\left[\frac{\gamma_{\mathrm{L}}^{\mathrm{d}}\gamma_{\mathrm{s}}^{\mathrm{d}}}{\gamma_{\mathrm{L}}^{\mathrm{d}} + \gamma_{\mathrm{s}}^{\mathrm{d}}} + \frac{\gamma_{\mathrm{L}}^{\mathrm{p}}\gamma_{\mathrm{s}}^{\mathrm{p}}}{\gamma_{\mathrm{L}}^{\mathrm{p}} + \gamma_{\mathrm{s}}^{\mathrm{p}}}\right] \tag{2.4}$$

The surface energy of the solid γ_s and its two components γ_s^d and γ_s^p are calculated using equation 2.4 and contact angle data for two liquids with known values for γ_L, where one of the liquids should be polar and the other liquid non-polar. This is described by equation 2.5, where *i* denotes the two liquids.

$$\gamma_{\mathrm{i}}(1 + \cos\theta_{\mathrm{i}}) = 4\left[\frac{\gamma_{\mathrm{i}}^{\mathrm{d}}\gamma_{\mathrm{s}}^{\mathrm{d}}}{\gamma_{\mathrm{i}}^{\mathrm{d}} + \gamma_{\mathrm{s}}^{\mathrm{d}}} + \frac{\gamma_{\mathrm{i}}^{\mathrm{p}}\gamma_{\mathrm{s}}^{\mathrm{p}}}{\gamma_{\mathrm{i}}^{\mathrm{p}} + \gamma_{\mathrm{s}}^{\mathrm{p}}}\right] \quad ; \mathrm{i} = 1, 2 \tag{2.5}$$

where;

$$\gamma_{\mathrm{i}} = \gamma_{\mathrm{i}}^{\mathrm{d}} + \gamma_{\mathrm{i}}^{\mathrm{p}} \quad ; \mathrm{i} = 1, 2$$
$$\gamma_{\mathrm{s}} = \gamma_{\mathrm{s}}^{\mathrm{d}} + \gamma_{\mathrm{s}}^{\mathrm{p}}$$

θ_i: contact angle of liquid *i*
γ_i: surface energy of liquid *i*
γ_i^d, γ_i^p: dispersion and polar energy of liquid *i*
γ_s^d, γ_s^p: dispersion and polar energy of surface

The contact angle on a solid surface could be measured using the sessile drop method. A drop of a liquid with known surface energy is placed on a surface and the contact angle is measured [4]. In the most basic way this could be done with a goniometer, where the drop is viewed and estimated by ocular inspection. More common today, and used in this project, is to capture the picture with a digital camera and export it into a computer program where the contact angle and also the surface energy are evaluated by a suitable software.

2.2 Pre-treatment

Two main reasons for pre-treatment of polymeric surfaces prior to bonding is the removal of contaminants (e.g. mold release, oil, or fingerprints) and to increase the surface energy to enable wetting [4] [20], i.e. a low contact angle. This is often referred to as surface cleaning and activation. In the following two subchapters the pre-treatments used in this project are presented.

2.2.1 Solvent wiping

Solvent wiping is the simple process of wiping the surface with a cloth immersed in a solvent. The aim is to dissolve and evaporate the contaminants using the solvent. The use of solvents in the industry is restricted due to safety and health regulations [3]. However, solvent wiping could only achieve one of the two main reasons mentioned above, cleaning. It does not increase the surface energy [4] and there is also a risk that the contaminants are simply distributed over the surface instead of removed [21].

2.2.2 Atmospheric pressure plasma treatment

The term plasma is often referred to as the fourth state of matter [5]. A plasma state occurs when a gas is energised such that it is fully or partially ionised. Examples of constituents in plasma are electrons, ions, free radicals, atoms, and molecules [6].

Plasma can be divided into two categories, thermal or non-thermal, also known as hot or cold plasma. The thermal plasma is in thermodynamic equilibrium, meaning that the electrons and the other species in the plasma are close in temperature. This gives rise to an overall high temperature, commonly of several thousand degrees Celsius. In non-thermal plasmas, the electrons have a high temperature but the other constituents are of approximately room temperature, causing the overall temperature to be considered as low. The non-thermal plasmas are used for surface treatment of polymers and could be produced both at low pressure (vacuum plasma) and at atmospheric pressure [5] [6].

For industrially used plasmas, a gas is exited to the plasma state by electrical discharge between two electrodes. In a remote type of surface treatment, as used in this project, the ionised gas is then directed through a nozzle towards the surface to be treated. The interaction of the plasma species with the surface can either remove or add particles to the surface. The former process is related to cleaning and etching of the surface, whereby contaminants or bulk material is removed. An example on the latter case is formation of oxygen containing groups e.g. –OH, –C=O and –COOH on the surface, which will enhance the surface energy. This is known as surface activation, however the effect is not permanent since the added groups tends to reorient themselves over time. [5] [6].

3 Materials and methods

The following chapter describes the materials and the methodologies used in the project.

3.1 Materials and equipments

In these subchapters the material and equipments used are listed and described. First the two kinds of pre-treatments used are presented. This is followed by a presentation of the substrate and the procedure for contaminating the substrate. The choice of adhesives is then motivated, followed by description of the measuring equipments.

3.1.1 Atmospheric pressure plasma set-up

The plasma equipment used was a Plasma-Dragon MAW produced by TIGRES GmbH. Only one nozzle was used, producing a free blowing plasma "flame", seen in Figure 3.1 a). The equipment worked at fixed power of 2 kW, the gas used was air at a pressure of 4 bars with a flow rate of 50 l/min. The nozzle head was mounted on an IRB2400/16 ABB robot to enable control of motion and repeatability of the plasma treatment, see Figure 3.1 b).

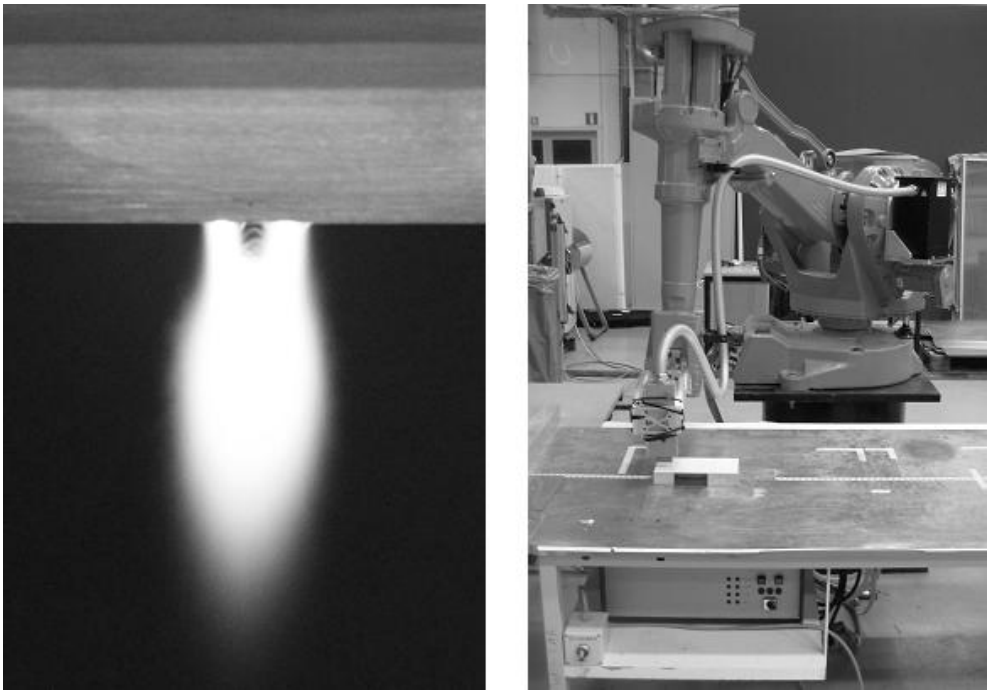

Figure 3.1: a) Picture of the free blowing plasma. b) Picture showing the plasma equipment mounted on robot at the set-up used during the project.

A program for the robot was used, causing a sweeping motion for the plasma nozzle, illustrated in Figure 3.2. In this program the variable parameters were treatment length, treatment width, speed, initial working distance, row distance, and increase of working distance/row. The treatment length and width were always set so that the whole substrate area was treated with parallel strokes and the turning motion into the next row was outside the substrate.

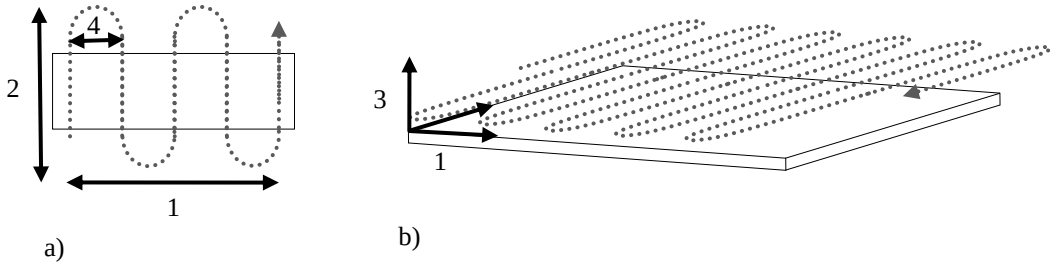

Figure 3.2: Schematic figures, a) from above b) 3D-view, describing the sweeping motion with the parameters, 1) treatment length, 2) treatment width, 3) working distance, 4) row distance.

3.1.2 Solvent wiping

Solvent wiping was used as a pre-treatment for two of the reference samples. It was conducted using a lint-free paper cloth immersed in a solution of equal volumes of water and isopropanol. The procedure was performed by wiping the surface with an unused immersed cloth seven times in the same direction.

3.1.3 Substrate

Painted steel plates supplied by VCC were used as substrate. The plates were received in a standard dimension of 100x200 mm. The paint system consisted of six layers, see Figure 3.3. The steel plates were first treated in the supplier's manufacturing process including phosphate conversion and electro-coating, the successive layers were then manually spray painted at VCC Surface Treatment Engineering department. The top clear coat was a high temperature-curing two-component polyester-urethane coating with isocyanate curing agent.

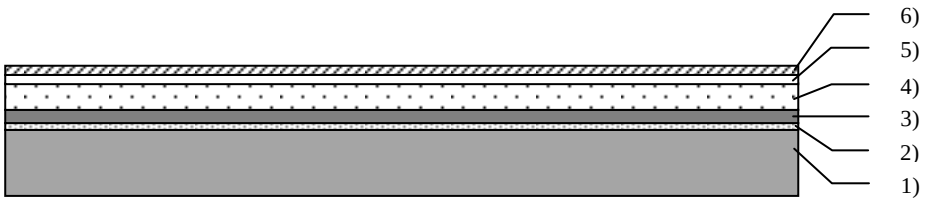

Figure 3.3: Schematic cross section of the painted steel plates. 1) Steel 2) Phosphate coat 3) Electro coat 4) Filler 5) Base coat 6) Clear coat

3.1.4 Contamination

To simulate a possible contamination that could be present on a painted car body in a production plant, an artificial soil called SebumTEFO was used. SebumTEFO consists of several ingredients where the main three are paraffin, palmic acid, and glyceryl tripalmitate.

Due to SebumTEFO being delivered as a solid, it had to be dissolved into a solution to enable even contamination of the substrate. In a first trial a small portion of SebumTEFO was put in isopropanol. After 48 h the soil had not dissolved, therefore cyclohexane was instead used to dissolve the soil instead.

A surface covered with fingerprints was decided to be a desirable level of contamination. The weight of a plate was recorded prior to and after being manually marked with fingerprints and the increase in weight was measured. Plates of the same size was then dipped in solutions of SebumTEFO in cyclohexane of different concentrations and let to air dry. A solution of 1 g sebum in 100 ml cyclohexane showed a similar weight increase as the plate covered in fingerprints. Hence, dipping the plate in the concentration of 1 g sebum in 100 ml cyclohexane, followed by evaporation of the solvent was chosen as a contamination procedure for the substrate.

3.1.5 Adhesives

VCC desired to use an adhesive foam tape for the experimental methods where the adhesive strength against the substrate were to be evaluated. 3M Acrylic Foam Tape GT 6012 F was chosen due to its similarity to an adhesive foam tape used in the industrial production for attachment of plastic details to the clear coat on the car body.

However, during the experimental part of the project problems with this tape occurred, see Chapter 3.2.5.2 Pull-off adhesion test. Therefore the choice was made to use an epoxy adhesive instead. 3M Scotch-Weld DP760 epoxy adhesive was used for the lap shear test specimens.

3.1.6 Contact angle measurement equipment

The equipment for performing static contact angle measurement and calculations of surface energy was a VCA2500 Video Contact Angle System from AST Products. Two liquids were used, deionised water and methylene iodide. The software AutoFast was used to determinate contact angles and the software SE-2500 to calculate the surface energy using the harmonic-mean method.

3.1.7 Pull-off adhesion test equipment

Adhesion tests were conducted using a manual hydraulic tensile adhesion tester model GM01 manufactured by Surftec. The equipment consists of a pressure source, a pressure gauge, an actuator and test elements, see Figure 3.4. The test elements used had a diameter of 14 mm.

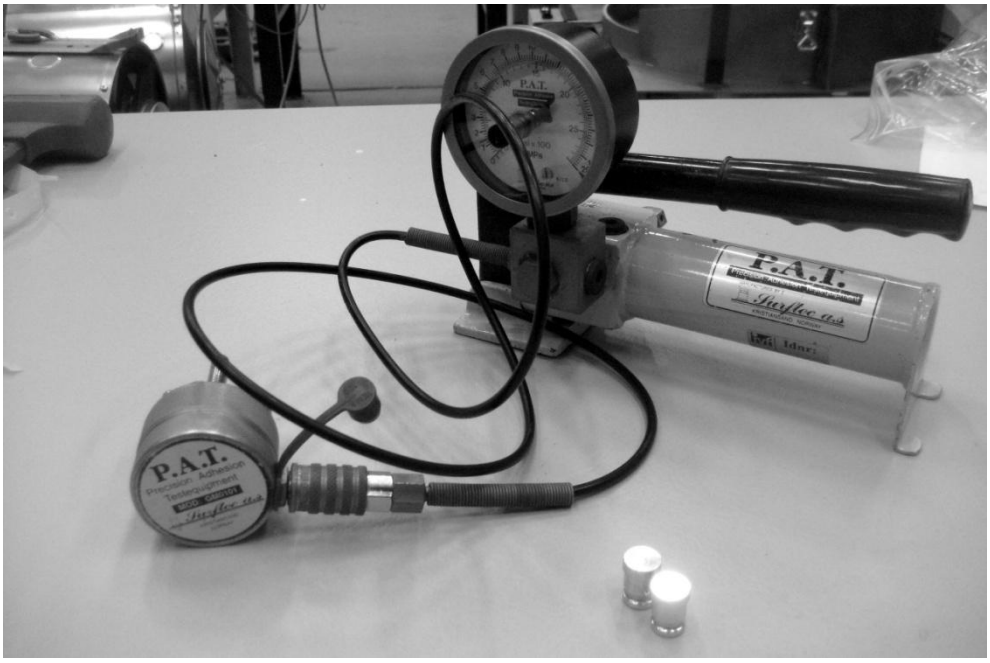

Figure 3.4: Picture of the pull-off adhesion test equipment, including two test elements.

3.1.8 Lap shear test equipment

The lap shear tests were conducted using a MTS M20 load frame with a load cell of 10kN. The test speed was 5.1 mm/min, all tests ran until the specimen broke and the peak load was registered.

3.2 Methods

The methodology used in the project could be divided into three parts, pre-evaluation, design of experiments (DOE), and preparation and conduction of experiments including measuring of the results.

Although a full factorial experiment of the atmospheric pressure plasma treatment was desired in the beginning of the project, the pre-evaluation of the plasma treatment parameters had to be done prior the DOE to enable setting of the levels for the speed and the working distance.

3.2.1 Pre-evaluation of plasma treatment parameters

In the set-up used, the amount of plasma treatment of an area depended on the distance from the nozzle to the substrate (working distance) and the exposure time. This means that a lower working distance or speed, or a combination of both, would result in a more intense treatment. Since there was no previous experience of this atmospheric pressure plasma set-up with this substrate, a pre-evaluation on how variations in speed and working distance would affect the surface energy of the substrate was conducted.

Three as received (AR) standard plates was used with the following parameters: speed: 50, 100, or 200 mm/s, initial working distance: 5 mm, increase of working distance/row: 5 mm, and row distance 25 mm. This resulted in seven rows per plate, working distances spanning from 5 to 35 mm, see Figure 3.5.

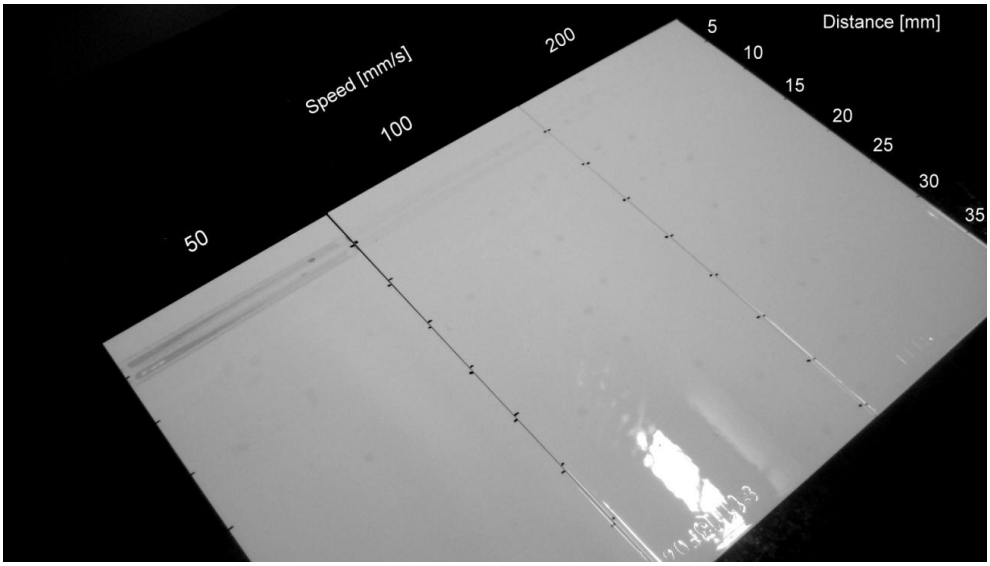

Figure 3.5: Picture of the three plates used in the pre-evaluation after the atmospheric plasma treatment. Burn marks are visible for the areas plasma treated at a working distance of 5 mm for 50 and 100 mm/s. the spots seen on the surfaces are due to the measurements liquids.

Two measurements of contact angles and calculations of surface energy were done for each row, the results can be found in Appendix I. The surface energy and the polar component of the surface energy together with visual inspection of the samples formed the decision basis for the chosen levels of speed and working distance.

The most intense parameters (5 mm and 50 mm/s) caused burn marks on the substrate and therefore these were chosen as the lower levels for the factors distance and speed. The increase in polar component of surface energy was most clear for the working distances from 5 to 25 mm. Thus 25 mm was chosen as the higher level for the factor working distance and 15 mm as a middle level. The speeds 100 and 200 mm/s showed similar effects on the surface energy; therefore these were set as middle and high levels.

The treatment width of one row depended on the width of the plasma flame, which varied with the working distance since the blown-out plasma was flame shaped. An even plasma treatment of the surface was desired, without overlapping treatment or untreated area between the treated rows. Therefore, the treatment width for the three different working distances was measured and the row distance for these three distances was set according to Table 3.1.

Table 3.1: Row distance set for the working distances used.

Working distance [mm]	Row distance [mm]
5	15
15	13
25	10

3.2.2 Design of experiments (DOE)

A total of three factors, i.e. input parameters, were selected; speed, working distance, and surface status. Speed and working distance were related to the plasma pre-treatment. Surface status was a factor used to describe the surface prior to eventual pre-treatment. Speed and working distance were set at three levels each, i.e. three variations per factor. These levels were set according to the pre-evaluation. The third parameter, surface status, was investigated on two levels; AR meaning that the substrate was not purposely contaminated, SebumTEFO meaning purposely contaminated according to the process described in Chapter 3.1.4 Contamination. This DOE resulted in 18 different combinations of the factors and their levels, which led to a test matrix with 18 different samples for a full factorial test, see Table 3.2.

Table 3.2: Test matrix, the samples are listed with their corresponding process parameters and surface status.

Sample No.	Working distance [mm]	Speed [mm/s]	Surface status
1	5	50	AR
2	5	50	SebumTEFO
3	5	100	AR
4	5	100	SebumTEFO
5	5	200	AR
6	5	200	SebumTEFO
7	15	50	AR
8	15	50	SebumTEFO
9	15	100	AR
10	15	100	SebumTEFO
11	15	200	AR
12	15	200	SebumTEFO
13	25	50	AR
14	25	50	SebumTEFO
15	25	100	AR
16	25	100	SebumTEFO
17	25	200	AR
18	25	200	SebumTEFO

The number of measurement replicates for each sample was set to five. A total of ten result parameters were chosen. Out of these ten, the main three were surface energy, peak stress, and peak load. The experimental methods and their corresponding result parameters, amount of specimens for each sample and measurements per specimen are listed in Table 3.3.

Table 3.3: Experimental methods and result parameters

Experimental method	Result parameters	Specimen/ sample	Measurements /specimen
Contact angle measurement	Surface energy, polar component of surface energy	1	5
Pull-off adhesion test	Peak stress, failure mode (in terms of percentages adhesive, cohesive and paint failure)	1	5
Tensile lap shear test	Peak load, failure mode (in terms of percentages adhesive, cohesive and paint failure)	5	1

3.2.3 Reference samples

For the comparison between the atmospheric pressure plasma treatment, solvent wiping and a non pre-treated substrate, four reference samples were prepared according to Table 3.4. The number of specimens per sample, experimental methods and measurements were performed in the same way as for the plasma-treated samples.

Table 3.4: Reference samples, their sample number and corresponding surface status and pre-treatment

Sample No.	Pre-treatment	Surface status
19	None	AR
20	None	SebumTEFO
21	Solvent wiping	AR
22	Solvent wiping	SebumTEFO

3.2.4 Specimen preparation

The substrate was cut in dimensions adjusted to the corresponding experimental method, according to Table 3.5.

Table 3.5: Specimen dimensions for the experimental methods.

Experimental method	Specimen dimension [mm]
Contact angle measurement	100x200
Pull-off adhesion test	100x100
Tensile lap Shear test	2.5x100

If SebumTEFO was set as surfaces status for the sample, the corresponding specimen/specimens was contaminated as described in Chapter 3.1.4 Contamination. Figure 3.6 shows the visual difference between a contaminated and a non-contaminated surface, surface status SebumTEFO and AR respectively.

All specimens were stored at 23 °C and 50 % RH for at least 48 h before eventual pre-treatment and measurements were performed.

Figure 3.6: Picture of two standard plates with different surface status, to the left SebumTEFO, to the right AR. Note the difference in light reflection.

Pre-treatment

Samples no. 1 to 18 were pre-treated with atmospheric plasma treatment, with parameters according to the test matrix, Table 3.2. Samples 19 and 20 were not pre-treated. Samples 21 and 22 were solvent-wiped using the procedure described in Chapter 3.1.2 Solvent wiping.

3.2.5 Experimental methods

The following subchapters describe how the three types of measurements were carried out in order to obtain the response parameters. For the pre-treated samples (all except samples no. 19 and 20), the measurements were carried out directly after the pre-treatment.

3.2.5.1 Contact angle measurement and calculation of the surface energy

Five measurements were done for each specimen. The drops were dispensed manually with a syringe. The mean drop volumes were 0.693±0.145 µl and 1.519±1.130 µl for deionised water and methylene iodide, respectively. The drops had a wetting time of 3 seconds before the contact angles, left and right angles, of the drop were determined. The contact angle data was then used to calculate the surface energy by the software SE-2500, using the harmonic-mean method.

3.2.5.2 Pull-off adhesion test

GT 6012 F 3M Acrylic Foam Tape was applied to the test elements and left for conditioning for two weeks. Five test elements were then mounted on each specimen, see Figure 3.7, and stored at 23 °C and 50 % RH for one week. The test was conducted by fastening the actuator to the test element, force was then applied until the test element was pulled off. This test procedure was performed, but no conclusive results could be read on the pressure gauge. This is suspected to be due to the viscoelasticity of the foam. Despite additional test procedures where specimens where frozen in an attempt to stiffen the foam, no results were obtained. Therefore, this experimental method was rejected and the result parameter peak stress was not used.

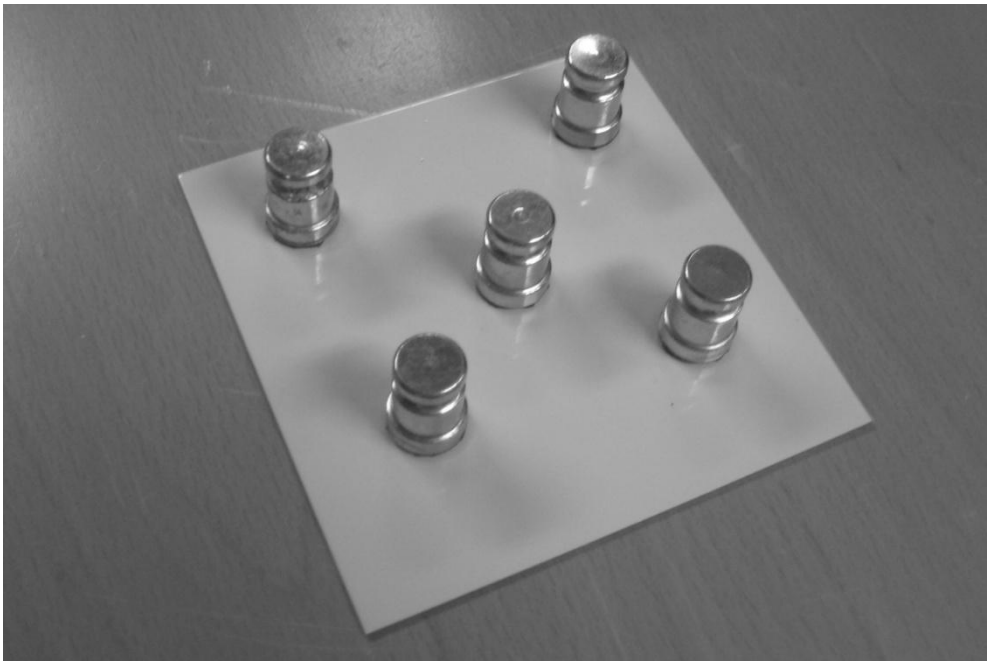

Figure 3.7: Five test elements mounted on a specimen.

3.2.5.3 Tensile lap shear test

Fixtures as the one seen in Figure 3.8 was used to create lap shear test specimens with the geometry shown in Figure 3.9. Strips of polytetrafluoroethylene with a thickness of 0.2 mm was used to control the thickness and delimit the area of the adhesive. The epoxy adhesive 3M Scotch-Weld DP760 was applied and the specimens were put together and tightened using wing nuts. The curing cycle was 24 h in room temperature followed by 48 h at 45 ˚C. The specimens were then stored at 23 ˚C and 50 % RH for 24 h before demounted from the fixture. Possible excessive adhesive that had cured on the edges of the specimens were removed by grinding.

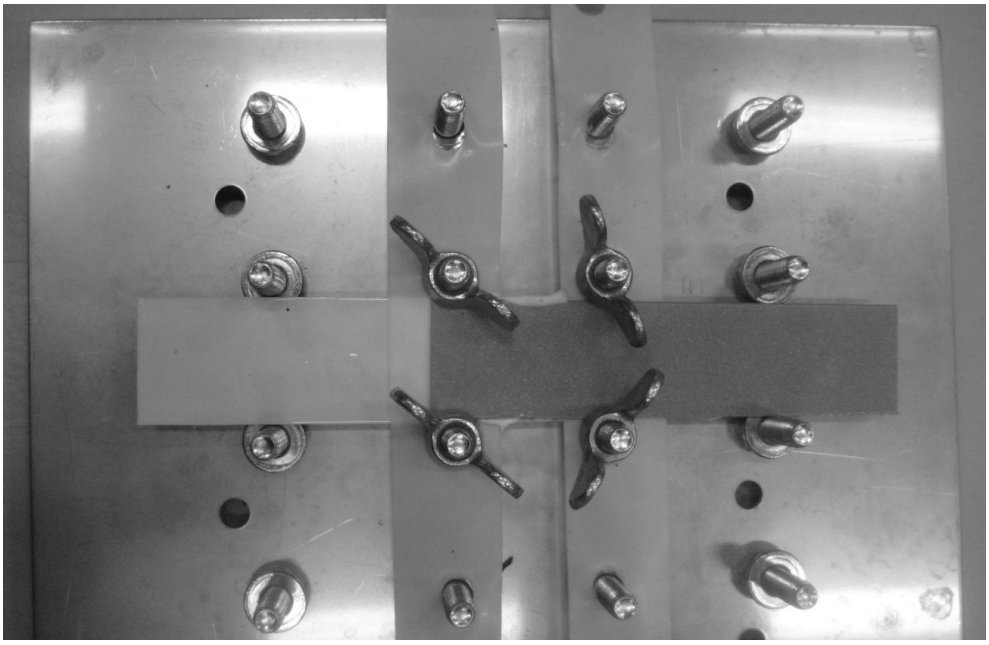

Figure 3.8: Picture of one specimen placed and tightened in the fixture.

The tests were conducted by placing the specimen in the load frame. The test procedure was set to run at a speed of 5.1 mm/min until the specimen broke. The peak load was registered for each specimen.

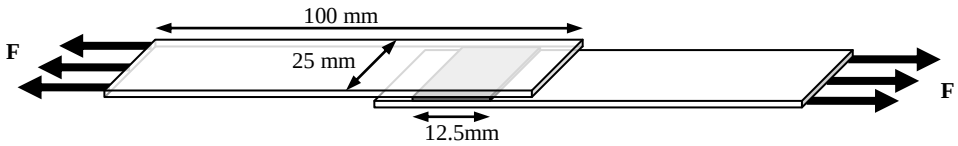

Figure 3.9: Schematic figure showing the geometry of the lap shear test specimens.

Each specimen was visually evaluated using a raster to determine percentages of failure modes (Figure 3.10). Three types of failure mode where available, adhesive, cohesive and paint failure. The failure mode was set as adhesive if the clear coat could be seen as unaffected. If any adhesive remained of the substrate the mode was determined as cohesive, meaning the fracture had progressed inside the adhesive. Paint failure mode was set if any of the paint layers beneath the clear coat was visible.

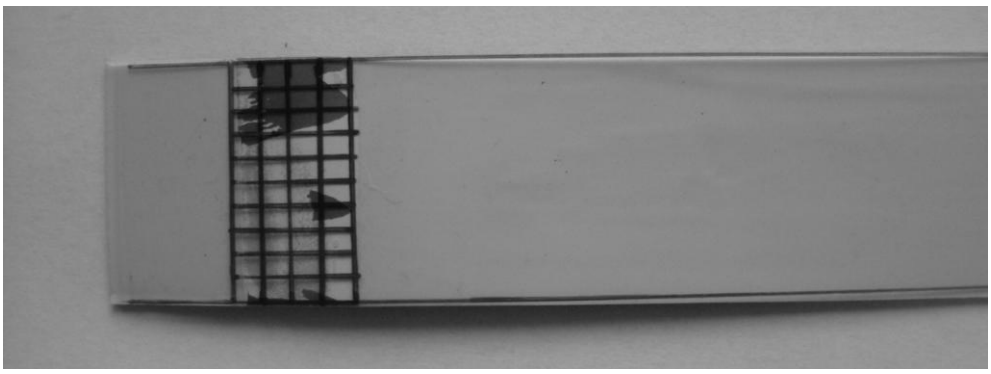

Figure 3.10: Raster positioned on top of a specimen.

3.2.6 Data analysis

The obtained data from the experiments was divided into three groups; reference samples (sample 19-22), AR-samples (sample 1, 3, 5, 7, 9, 11, 13, 15, and 17), SebumTEFO-samples (sample 2, 4, 6, 8, 10, 12, 14, 16, and 18).

The software Excel from Microsoft was used to visualise the data for surface energy, polar component, dispersive component, peak load and failure modes. Response surfaces for the response parameter peak load were created using the statistical software Minitab 16 from Minitab Inc. This was done for the AR-samples and the SebumTEFO-samples. Correlations between the response parameters surface energy and peak load were also investigated.

4 Results

In this chapter the results from the experiments that were performed are presented. The results are the mean of five measurements per sample. The complete data is listed in the Appendix II.

4.1 Surface energy

The average surface energy calculated from contact angle measurements, including polar and dispersive components, for each sample is shown in Figure 4.1 to 4.3. The sample number and the corresponding mean value of the surface energy including its two components, are given on the x and y axis, respectively. The error bars represent one standard deviation.

Figure 4.1 illustrates the surface energies for the reference samples. Below the sample number, the possible pre-treatment and the surface status are given in parenthesis. The reference samples had a surface energy between 42 and 55 mJ/m².

Sample no. 19 had a surface energy of 47 mJ/m² with a polar component < 10 mJ/m². Sample no. 21, which had the same surface status as sample no. 19 but was pre-treated using solvent wiping, had a surface energy of 42 mJ/m². This sample had a lower dispersive component and a slightly higher polar component compared to sample no. 19. However, the variation of the polar component was higher for sample no. 21.

Sample no. 20 had a surface energy of 42 mJ/m², including a polar component of 14 mJ/m². Compared to sample no.19, sample no. 20 had a lower dispersive component but a slightly higher polar component. Sample 22 had a surface energy of 55 mJ/m² with a polar component of 19 mJ/m², which was the highest within this sample group.

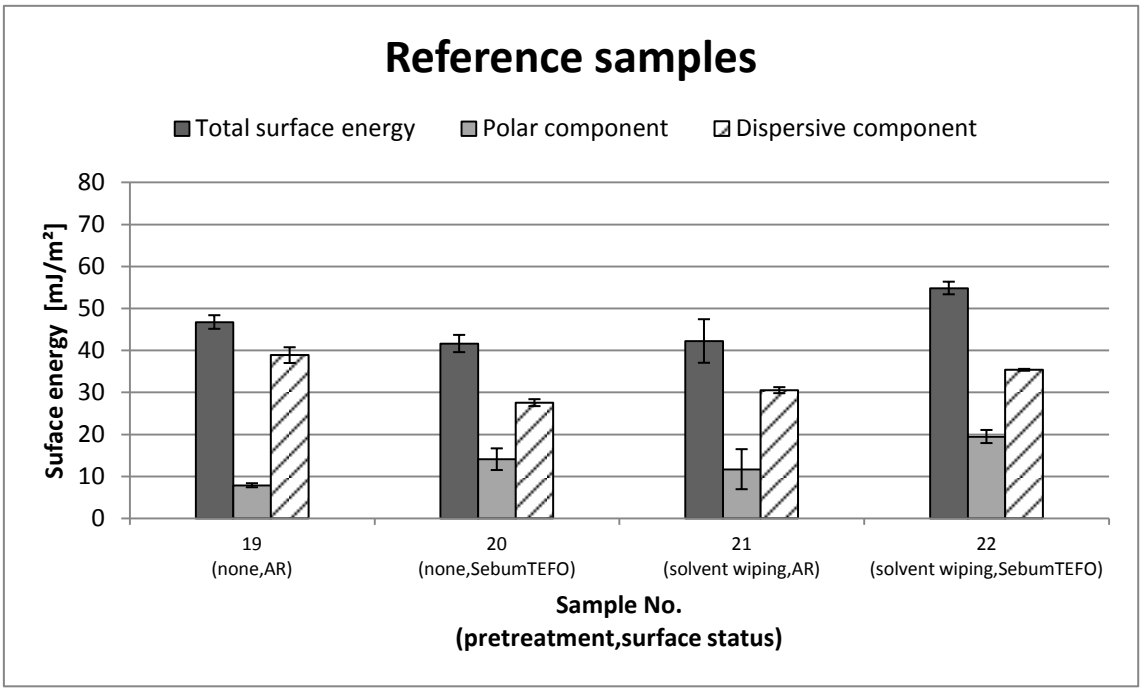

Figure 4.1: Surface energy of the reference samples.

The measured surface energies for the plasma treated samples, i.e. the AR-samples and the SebumTEFO-samples, are illustrated in Figure 4.2and Figure 4.3, respectively. Below the sample number, the parameters speed and working distance used are given in parenthesis.

The AR-samples had a surface energy between 46-70 mJ/m², except samples no. 15 and 17 which both had a surface energy < 35 mJ/m². Within this sample group the dispersive component ranged between 25 and 38 mJ/m² and the polar component varied between 6 and 34 mJ/m².

Sample no. 1 and 3, which were plasma treated with the two most intense process parameter settings (working distance 5mm and speed 50 or 100 mm/s), had a surface energy of 46 and 57 mJ/m², respectively

Surface energies > 60 mJ/m² was obtained for sample no. 5, 7, 9, and 11. These samples also had a polar component of > 25 mJ/m². However, sample no. 5 and 7 had a higher variation of surface energy compared to sample no. 9 and 11. The intensity of the plasma treatment of these samples was considered to be at an intermediate level.

A more mild plasma treatment, with a working distance of 25 mm, was used for sample no. 13, 15, and 17. Sample no: 13 had a surface energy of 53 mJ/m² with a polar component of 19 mJ/m², similar to sample no. 1 and 3. Sample no. 15 and 17 had the lowest surface energy within the sample group AR-samples, 35 and 31 mJ/m², respectively. Their polar components were similar to the polar components for the reference samples that had AR as surface status, sample no. 19 and 21.

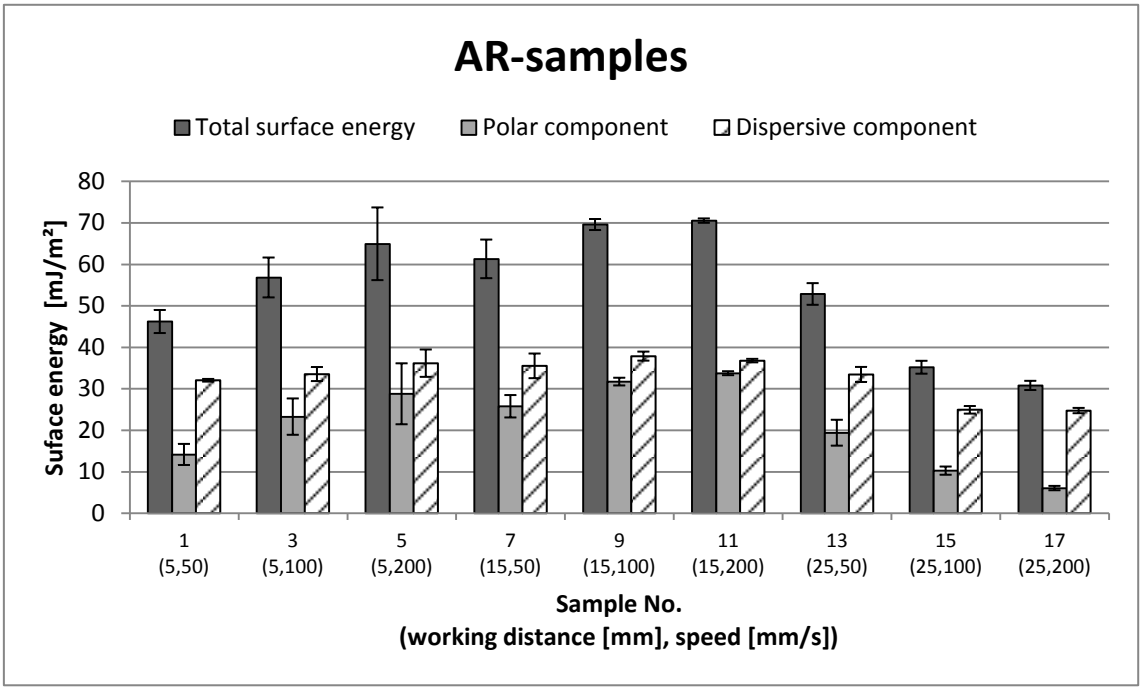

Figure 4.2: Surface energy of the AR-samples.

The SebumTEFO-samples had a surface energy between 45-64 mJ/m². Within this sample group the dispersive component ranged between 31 and 38 mJ/m² and the polar component varied between 12 and 30 mJ/m².

Sample no. 2, which had the most intense plasma treatment, had a surface energy of 46 mJ/m² with a polar component of 15 mJ/m². Surface energies > 60 mJ/m², including a polar component > 25 mJ/m², was obtained for samples no. 4 and 6. Sample no. 8 had a similar surface energy as sample no. 4 and 6, just a slightly lower polar component (24 mJ/m²) which resulted in a somewhat lower surface energy (58 mJ/m²).Sample no. 10, 12, 14, and 16, which had a intermediate to mild treatment level, had similar surface energies about 52-45 mJ/m². The mildest plasma treated sample, sample no. 18, had a surface energy of 45 mJ/m² with a polar component of 12 mJ/m². This was similar to the untreated reference sample that had SebumTEFO as surface status, sample no. 20.

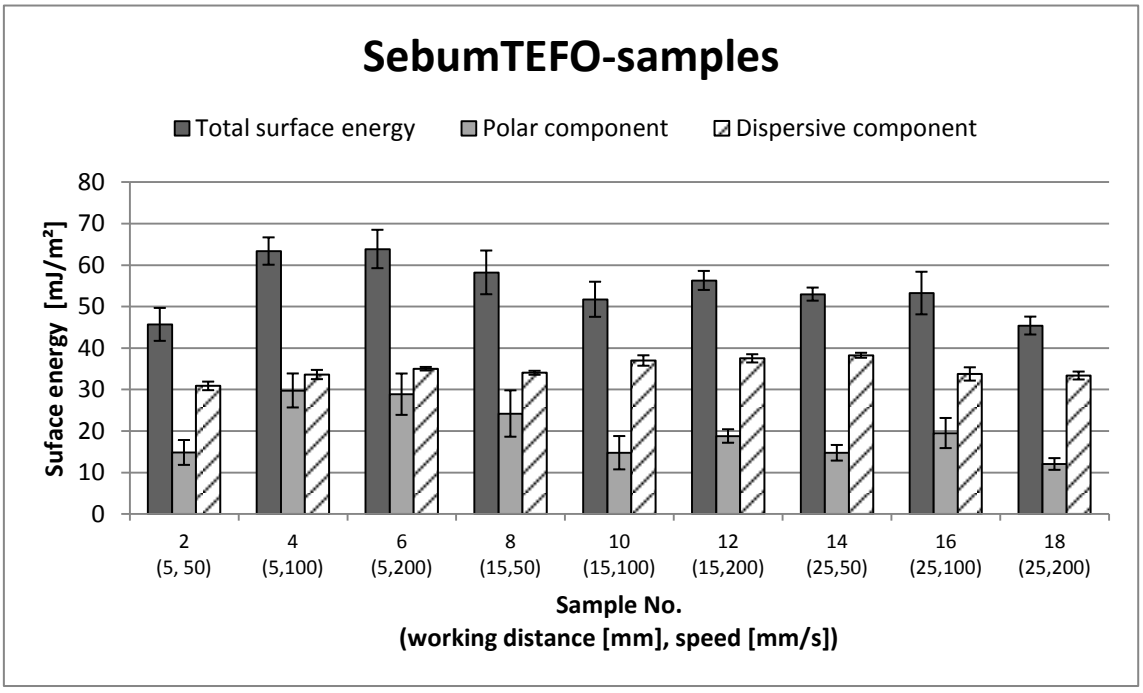

Figure 4.3: Surface energy of the SebumTEFO-samples.

4.2 Lap shear peak load

The mean peak load and the percentages of failure mode types for each sample are shown in Figures 4.4 to 4.6. The sample numbers are listed on the x-axis. Below the sample number the pre-treatment and the surface status are written in parenthesis for the reference-samples, for the AR-samples and the SebumTEFO-samples the parameters speed and working distance used are written in parenthesis. The primary axis corresponds to the mean peak load and the secondary axis to the percentages of failure mode. The error bars represent one standard deviation for the peak load results.

Since the values of failure mode types of a sample are the average out of five specimens, this could be somewhat misleading when the specimens within a sample differed greatly. For example, sample no. 14 in Figure 4.6 exibited a mean of 45 % adhesive failure mode. Within this sample one specimen had 100 % adhesive failure mode and another specimen only 12.5 %. This could be seen in the complete data, listed in Appendix II.

Generally, if the degree of adhesive failure of a sample is high, the peak load could be seen as a measurement of the bond strength between the adhesive and the clear coat. If a sample has a large proportion of paint failure, the peak load does not measure the bond strength between adhesive and clear coat. It could only be stated that the adhesive bond was stronger than the cohesive strength of the paint system. The cohesive failure mode was rarely observed.

All reference samples exhibited 100 % adhesive failure mode, see Figure 4.4. The samples pre-treated with solvent wiping showed a similar peak load as those that were not pre-treated. Compare sample no.19 to no.21 that had a peak load of about 1.85 kN and sample no. 20 to no. 22 that had a peak load of about 0.5 kN. Hence, solvent wiping did not affect the peak load of the samples. However, the effect of contamination was clearly seen, the uncontaminated samples (sample no. 19 and 21) had a peak load about three to four times higher than the contaminated samples (sample no. 20 and 22).

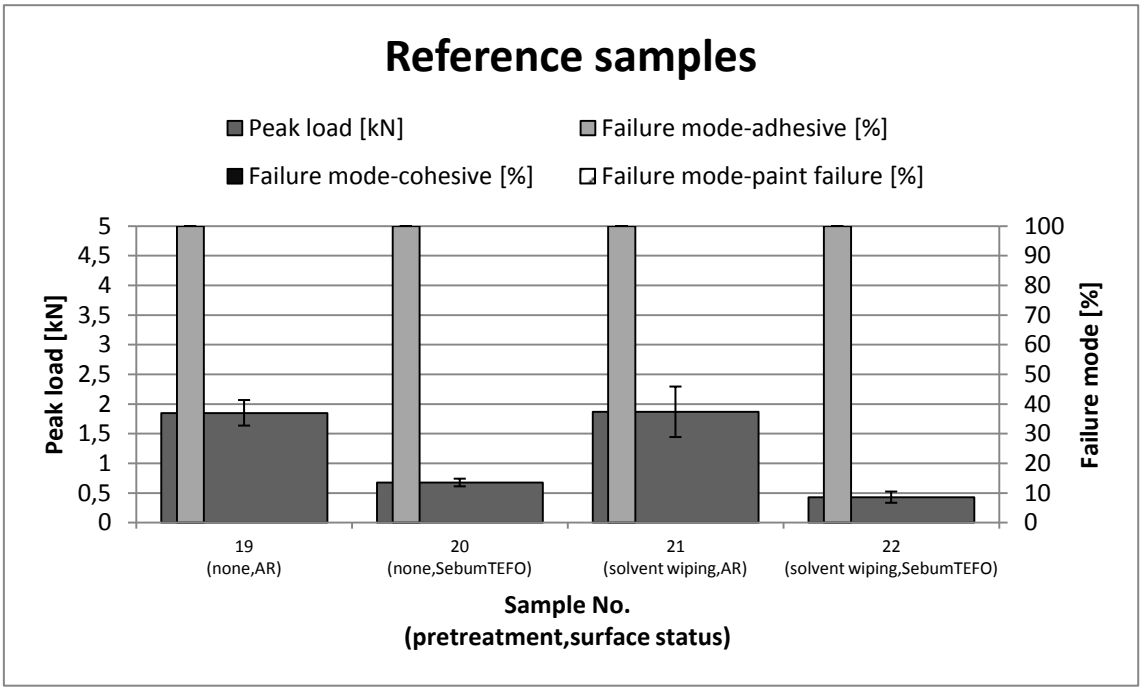

Figure 4.4: Peak load registered during the lap-shear test and evaluated percentages of failure mode for the reference samples.

All the AR-samples showed similar results, with peak loads from 3.2 kN up to 3.8 kN and high percentages of the failure mode paint failure, see Figure 4.5. In general, the peak load of the AR-samples were almost two times higher than that of the reference samples that had AR as surface status (sample no. 19 and 21).

The intermediate to mild plasma treated samples (sample no. 7, 9, 11, 13, 15, and 17) had a peak load > 3.5 kN. Sample no. 15 had the highest peak load, 3.8 kN, and also very little variation within the sample. The samples that were plasma treated with a working distance of 5 mm (sample no. 1, 3, and 5) had slightly lower peak loads, spanning from 3.25 to 3.45 kN.

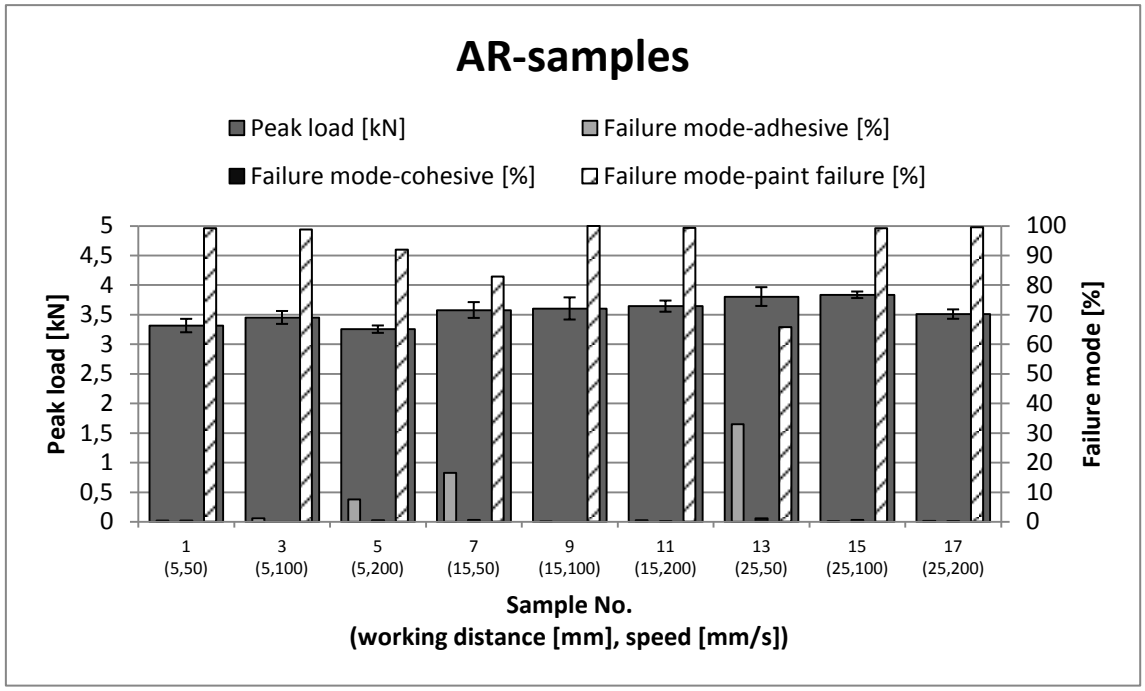

Figure 4.5: Peak load registered during the lap-shear test and evaluated percentages of failure mode for the AR-samples.

The SebumTEFO-samples had peak loads spanning from 1.2 to 3.4 kN with various types of failure modes, see Figure 4.6. Except for sample no. 14, there was a tendency that a more intense plasma treatment, shorter working distance and speed, resulted in a higher peak load. Sample no.2 had the highest peak load (4.3 kN), the lowest variation within a sample and the highest percentages of paint failure within the group. Sample no. 4 and 6, which also had a working distance of 5 mm, had a peak load of 3.3 and 3 kN, respectively.

Sample no. 8 and 14, which both had a plasma treatment speed of 50 mm/s, showed a peak load of 2.2 and 2.9 kN, respectively. However, sample no. 14 showed large variation. This depended on a single sample which had a significantly lower peak load, see Appendix II. Sample no. 10, 12, 16, and 18, which were plasma treated on a intermediate to mild level, had peak loads < 2kN and high percentages of adhesive failure mode.

Only two of the SebumTEFO-samples (samples no. 2 and 4) had a peak load higher than the lowest peak load for the AR-samples (sample no.5). However, all of the SebumTEFO-samples had a higher peak load than the two reference samples that had SebumTEFO as surface status (sample no. 20 and 22).

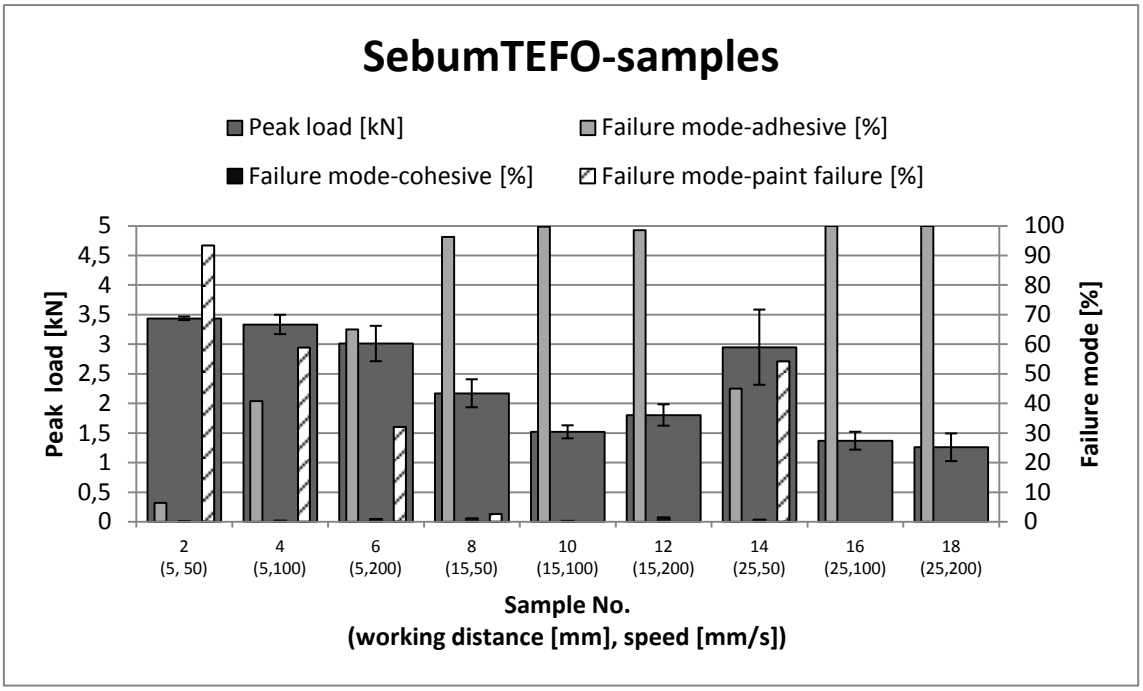

Figure 4.6: Peak load registered during the lap-shear test and evaluated percentages of failure mode for the SebumTEFO-samples.

Response surfaces

Figure 4.7 and Figure 4.8 shows the response surface for the AR-samples and the SebumTEFO-samples, respectively. These graphs were created by setting the factors speed and working distance, including their levels, as input. The measured peak load was set as the response parameter. These figures contain the same results as Figure 4.5 and Figure 4.6, together with interpolations made by the software Minitab 16. The response surface design is available in the Appendix III. Note the difference in z-axis scale in the two figures.

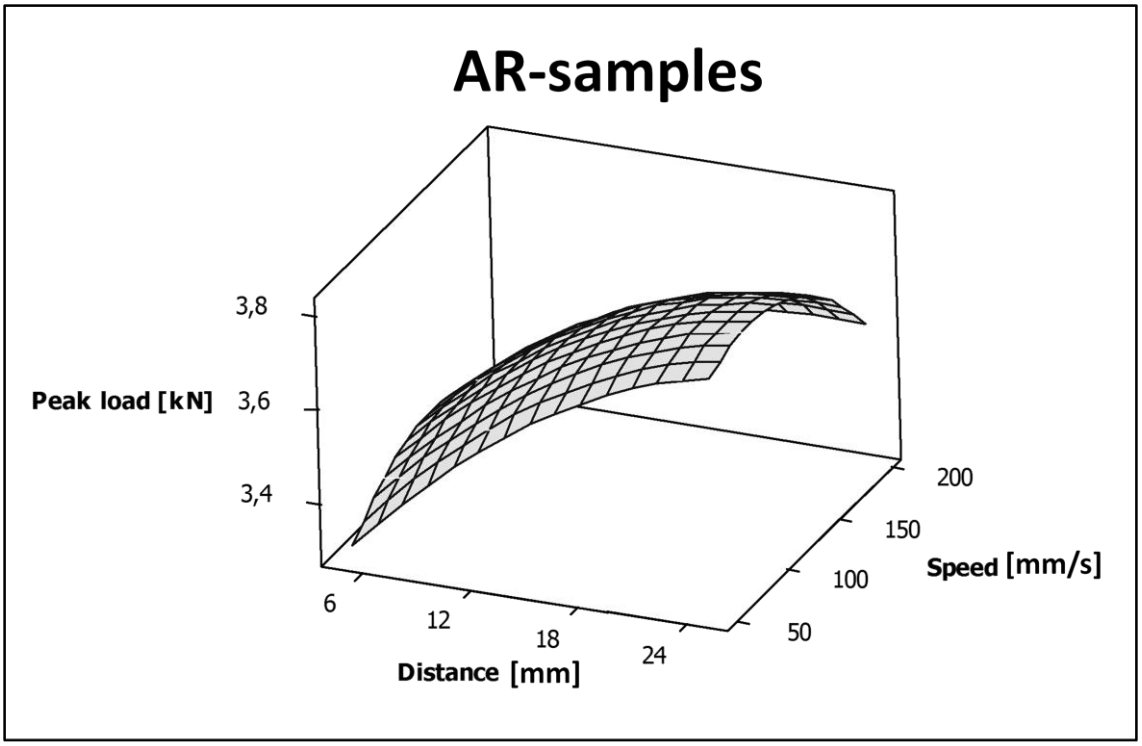

Figure 4.7: Response surface for the AR-samples.

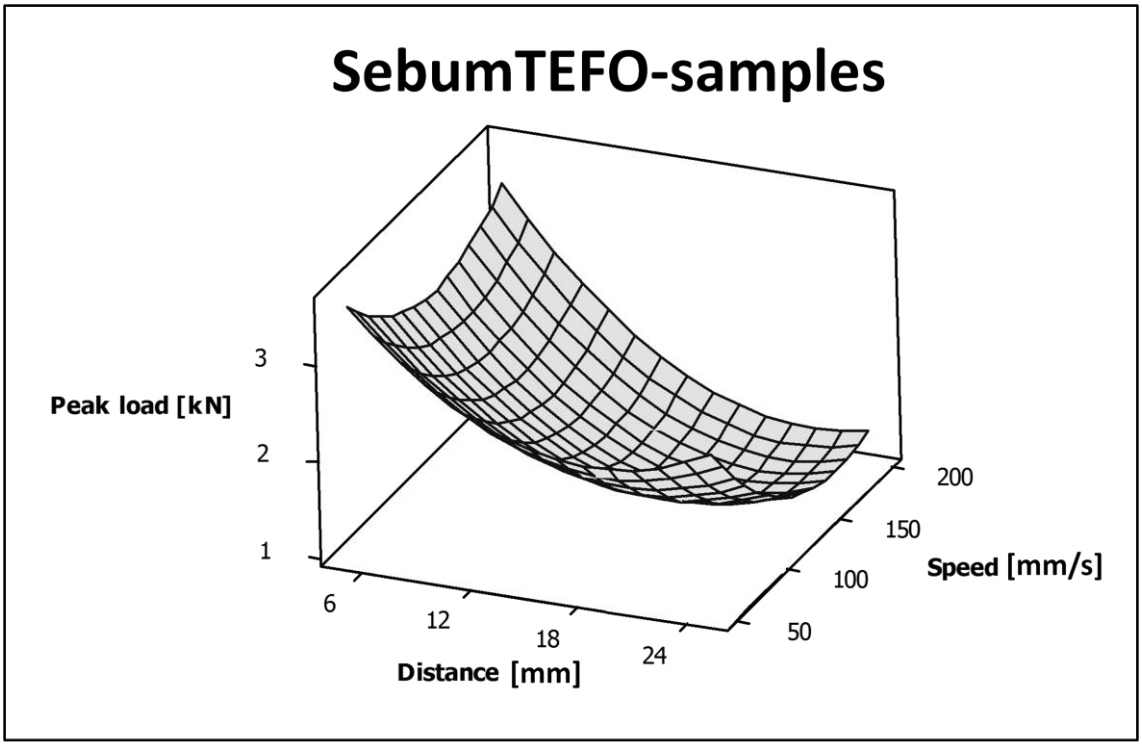

Figure 4.8: Response surface for the SebumTEFO-samples.

From Figure 4.7 it is obvious that the highest peak load is obtained for a speed of about 100-150 mm/s and a working distance of 15 mm or more. However, the response in peak load did not vary more than 0.6 kN within the sample group AR-samples.

In Figure 4.8 the response surface resembles a hammock with three local maxima and a valley. Disregarding one of the maxima where the response in peak load is about 2 kN, the other two maximum points located at a working distance equal to about 5 mm. Hence, a peak load of 3 kN or more is obtained for a working distance of 5 mm, irrespective of speed within the range of 50-200 mm/s.

4.3 Correlation between surface energy and lap shear peak load

The mean surface energy plotted against the mean lap shear peak load for the AR-samples and the SebumTEFO-samples is displayed in Figure 4.9. None of the two sample groups showed any correlation between the surface energy and the peak load.

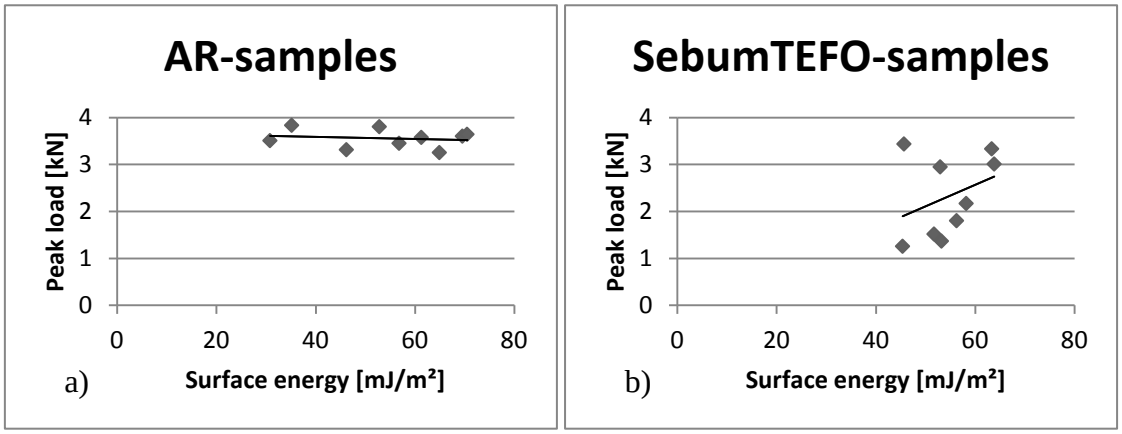

Figure 4.9: The mean surface energy as a function of the mean lap shear peak load for, a) the AR-samples and b) the SebumTEFO-samples.

5 Discussion

This chapter includes reflections and interpretations of the results. Problems that occurred during the project and possible error sources are also discussed. Suggestions for future work are also mentioned.

Results

The results indicate that an enhancement of both the surface energy and the adhesion is possible using atmospheric pressure plasma treatment. However the results depend on the process parameter settings and the surface status.

When discussing differences in surface energy it should be taken in consideration that only large differences could be seen as significant. This is due to the possible variance in the measurement method used, contact angle measurement. The variance in surface energy was most seen as the variance in the polar component. The dispersive component exhibited in general a low standard deviation. The largest standard deviations were calculated for sample no. 5, 7.3 mJ/m² and 3.3 mJ/m² for the polar and the dispersive component, respectively.

The surface energies of the four reference samples were similar. This indicates that using solvent wiping did not affect the surface energy, which was also was mentioned in the theory. Noticeable is that the contaminated samples did not exhibit significantly lower surface energies than the ones without contamination. Instead, the polar component seemed to have been enhanced by the contamination. This might be related to the contamination process or due to the ingredients in the soil used for contamination.

Comparing the surface energies of both the AR-samples and the SebumTEFO- samples, only one plasma process parameter setting, working distance: 5 mm, speed: 200 mm/s, resulted in similar and fairly high surface energies for the two sample groups. This indicates that this parameter setting would be favourable to use, in terms of surface energy, in a case of an unknown surface status of the substrate in an industrial production environment. However, this setting is a compromise since there were others that resulted in higher surface energies for the AR-samples.

A correlation between the two result parameters surface energy and peak load was not found, neither for the AR-samples nor for the SebumTEFO-samples. This might be a consequence of the adhesive being too good at bonding to these surfaces. However, the adhesive seemed affected by the contamination, since in general, the samples that had SebumTEFO as surface status in general had lover peak loads than the ones that had AR as surface status.

Cohesive failure mode was almost never observed and could have been excluded as a result parameter. The reason that it rarely, if ever occurred is most probably due to the stiffness or strength of the adhesive. The fact that the colour of the adhesive was similar to the colour of the substrate also complicated the assessment.

The standard deviation of the peak load results for the AR-samples was about 0.11 kN, with the largest being 0.19 kN for sample no. 13.The SebumTEFO-samples had higher variance in peak load with a standard deviation of about 0.4 kN, except sample no. 2 which had a standard deviation of 0.03 kN. This small variance may be due to the intense plasma treatment, removing a lot of the SebumTEFO on the surface. The largest variance was seen for sample no. 14, which had a standard deviation of 1.8 kN.

Comparing the plasma-treated AR-samples to the non-pre-treated and solvent-wiped reference samples with AR as surface status, it is seen that all the plasma-treated samples exhibited a higher peak load than any of the two reference-samples. The same applies when comparing the plasma-treated SebumTEFO-samples to the two reference samples with surface status SebumTEFO. This indicates that any plasma treatment is better than no pre-treatment or solvent wiping.

Comparing the peak loads of both the AR-samples and the SebumTEFO- samples, only one plasma parameter setting, distance: 5 mm, speed: 50 mm/s, gave a similar peak load and high percentages of the failure mode paint failure. However, as seen in the pre-evaluation this parameter setting causes burn marks on the substrate if the surface status is AR. Therefore, this parameter setting would not be suitable to use in an industrial production environment where the status of the surface is unknown.

Experimental uncertainty and possible error sources

The major problem during this project was the contamination. The contamination process (dipping in soil solution) was not reliable and the reproducibility was considered to be low. A higher concentration of SebumTEFO was formed where the edge of the drops had been prior to evaporation of the solvent. This resulted in a more or less uneven distribution of the soil. Since the contamination was one input parameter to the test matrix and also used on two of the reference samples, this instability probably affected the result for all the contaminated samples.

Another issue was the amount of contamination. The purpose of the contamination was to simulate a surface filled with fingerprints. However, the actual outcome of dipping the samples in the solution was probably a more severe contamination. This made the SebumTEFO-samples less close to a realistic contamination situation, which gave less utility of the results from these samples.

The table used in the plasma set-up had a surface made of sheet steel. During usage of the plasma equipment, heat was accumulated in the steel sheet, causing it to buckle. The specimens were placed upon blocks of aluminium, used as spacers, in attempt to migrate the buckling problem. Still, this may affected the working distance, causing the substrate to be closer to the nozzle than intended.

The wetting time, from placement of the drop to measurement of contact angle, was about three seconds for all the measurements. This short time was chosen since a longer wetting time gave very flat drops that floated out of the measurement region in case of the high surface energy surfaces. A longer wetting time could however have been favourable in order to gain more stable contact angle measurements.

It could be remarked that the evaluation of failure modes is an assessment, made by one person, and could therefore not be said to be an absolute fact. The evaluation of the failure modes was used as a guide of whether the adhesive bond was the weakest interface in a specimen or not.

Future work

Another contamination process with lower amounts of contamination and a higher repeatability is necessary in order to obtain samples that are more realistic with regard to an industrial environment.

A surface analysis should be conducted in order to investigate which effect the plasma treatment has on the surface chemistry and topography. X-ray photoelectron spectroscopy could be used to detect possible oxygen groups introduced by the plasma treatment. The possible effect of plasma treatment on surface topography could be investigated by atomic force microscopy.

The shelf-life of the temporary surface activation effect could be investigated by conducting aging tests.

6 Conclusions

An atmospheric pressure plasma treatment and the set-up used in this project could be used as a pre-treatment for increasing the surface energy of the substrate and improve the adhesion. However, this was not achieved at a mutual process parameter setting. On the other hand, since no correlation between surface energy and adhesion was found, a process parameter setting giving a strong adhesion can be considered more important.

The lap-shear tests indicate a stronger adhesion due to the atmospheric pressure plasma treatment. However, with the amount of soil used for contamination in the project; a suitable set of the process parameters speed and working distance, for an unknown surface, more or less contaminated, could not be found. Further investigations are thus needed before implementation in a production environment.

7 References

[1] PlasticsEurope-Association of Plastic Manufacturers, “The Plastics Portal,” [Online]. Available: http://www.plasticseurope.org/use-of-plastics/transportation.aspx. [Accessed 14 05 2013].

[2] P. Mapleston, “Automotive plastics: an accelerating market,” *Plastics Engineering*, vol. 65, no. 5, pp. 10-12,14,16,18, 2008.

[3] R. A. Wolf, Atmospheric Pressure Plasma for Surface Modification, Somerset, NJ, USA : Wiley , 2012.

[4] A. V. Pocius, Adhesion and Adhesives Technology: An Introduction, 2 ed., Munich: Hanser Publishers, 2002.

[5] R. Shishoo, Plasma technologies for textiles, Cambridge: Woodhead Publishing Limited, 2007.

[6] H. Rausher, M. Perucca and G. Buyle, Plasma Technology for Hyperfunctional Surfaces, Weinheim: WILEY-VCH Verlag, 2010.

[7] M. Noeske, J. Degenhardt, S. Strudthoff and U. Lommatzsch, “Plasma jet treatment of five polymers at atmospheric pressure: surface modififations and the relevance for adhesion,” *International Journal of Adhesion & Adhesives,* vol. 24, no. 2, pp. 171-177, 2004.

[8] N. Encinas, B. Díaz-Benito, J. Abenojar and M. A. Martínez, “Extreme durability of wettability changes on polyolefin surfaces by atmospheric pressure plasma torch,” *Surface and Coatings Technology,* vol. 205, no. 2, pp. 396-402, 2010.

[9] M. D. Green, F. J. Guild and R. D. Adams, “Characterisation and comparison of industrially pre-treated homopolymer polypropylene, HF 135M,” *International Journal of Adhesion and Adhesives,* vol. 22, no. 1, pp. 81-90, 2002.

[10] H. Yaghoubi and N. Taghavinia, “Surface chemistry of atmospheric plasma modified polycarbonate substrates,” *Applied Surface Science,* vol. 257, no. 23, pp. 9836-9839, 2011.

[11] R. Stewart, V. Goodship, F. Guild, M. Green and J. Farrow, “Investigation and demonstration of the durability of air plasma pre-treatment on polypropylene automotive bumpers,” *International Journal of Adhesion and Adhesives,* vol. 25, no. 2, pp. 93-99, 2005.

[12] Vinnova, “Projekt finansierat av VINNOVA: PERU-Plasmabehandling för effektiv rutlimning,” 05 03 2013. [Online]. Available: http://www.vinnova.se/sv/Resultat/Projekt/Effekta/PERU-Plasmabehandling-for-effektiv-rutlimning/. [Accessed 14 05 2013].

[13] J. W. Gooch, Ed., Encyclopedic Dictionary of Polymers, 2 ed., vol. 1, Springer Science+Business Media, 2011.

[14] G. Fourche, “An overview of the basic aspects of polymer adhesion. Part I: Fundamentals,” *Polymer Engineering and Science,* vol. 35, no. 12, pp. 957-967, 1995.

[15] J. Schults and M. Nardin, “Theories and mechanisms of adhesion,” in *Handbook of Adhesive Technology,* A. Pizzi and K. L. Mittal, Eds., New York, Marcel Dekker, 2003, pp. 53-68.

[16] F. Awaja, M. Gilbert, G. Kelly, B. Fox and P. J. Pigram, “Adhesion of polymers,” *Progress in Polymer Science,* vol. 34, no. 9, pp. 948-968, 2009.

[17] D. E. Packham, “Theories of fundamental adhesion,” in *Handbook of Adhesion Technology,* L. F. M. da Silva, A. Ö. Öchsner and R. D. Adams, Eds., Berlin, Springer-Verlag, 2011, pp. 9-38.

[18] Casco Nobel AB, Industrilim, Limhandboken, Helsingborg: Casco Nobel AB, Industrilim, 1991.

[19] S. Wu, “Calculation of interfacial tension in polymer systems,” *Journal of Polymer Science Part C: Polymer Symposia,* vol. 34, no. 1, pp. 19-30, 1971.

[20] S. Ebnesajjad, Surface Treatment of Materials for Adhesion Bonding, New York: William Andrew Publishing, 2006.

[21] H. Karlsson, Limma med kvatlitet-en handbok, 2 ed., Mölndal: IVF Industriforskning och utveckling AB, 2001.

Appendix I Pre-evaluation data

The results obtained from the pre-evaluation of process parameters are presented in table (*referera*). The surface energy and its components are the mean value of two measurements.

Speed [mm/s]	Distance [mm]	Surface energy [mJ/m²]	Dispersive component	Polar component
50	5	63,5	33	30,5
50	10	73,9	42,1	31,8
50	15	71,9	42,8	29,1
50	20	62,3	36,2	26,1
50	25	52	33,7	18,3
50	30	37,3	30,1	7,2
50	35	35,3	28,8	6,5

Speed [mm/s]	Distance [mm]	Surface energy [mJ/m²]	Dispersive component	Polar component
100	5	62,5	34,6	27,9
100	10	76,6	43,5	33,1
100	15	71,4	37,1	34,3
100	20	65,4	32,6	32,8
100	25	35	24,7	10,3
100	30	30,1	24	6,1
100	35	33,1	26	7,1

Speed [mm/s]	Distance [mm]	Surface energy [mJ/m²]	Dispersive component	Polar component
200	5	69,6	33,2	36,4
200	10	71,9	36	35,9
200	15	69,4	35,4	34
200	20	39,6	26,1	13,5
200	25	31,5	25,7	5,8
200	30	29,8	22,6	7,2
200	35	39,2	31	8,2

Appendix II Experiment data

Sample	Specimen	Distance	Speed	Surface status	Dispersive comp. [mJ/m²]	Polar comp. [mJ/m²]	Surface energy [mJ/m²]	Lap Shear testing-Peak load [kN]	Lap Shear testing %-adhesive failure	Lap Shear testing %-cohesive failure	Lap Shear testing %-paint failure
1	1,1	5	50	0	32,1	12,2	44,3	3,423	1	1	98
	1,2	5	50	0	32	11,9	43,9	3,447	1	0,5	98,5
	1,3	5	50	0	31,5	12,6	44,1	3,271	0	0	100
	1,4	5	50	0	32,5	18,5	51	3,299	0	0	100
	1,5	5	50	0	32,1	15,6	47,7	3,133	0	0,5	99,5
3	3,1	5	100	0	31,2	28,3	59,5	3,252	0	0	100
	3,2	5	100	0	32,1	17,3	49,4	3,432	1,5	0	98,5
	3,3	5	100	0	33,8	19,3	53,1	3,487	0	0	100
	3,4	5	100	0	34,8	27,6	62,4	3,521	2	0	98
	3,5	5	100	0	35,8	23,9	59,7	3,567	2,5	0	97,5
5	5,1	5	200	0	34	32,5	66,5	3,259	0,5	0	99,5
	5,2	5	200	0	32,4	19	51,4	3,194	10	1	89
	5,3	5	200	0	39,5	21	60,5	3,184	5	0	95
	5,4	5	200	0	34,2	34,3	68,5	3,275	15	1	84
	5,5	5	200	0	40,7	37,1	77,8	3,357	7,5	0,5	92
7	7,1	15	50	0	31,3	28	59,3	3,391	10	0	90
	7,2	15	50	0	35,6	24	59,6	3,472	10	1,5	88,5
	7,3	15	50	0	34,1	22,8	56,9	3,61	7,5	0	92,5
	7,4	15	50	0	40,4	29,9	70,3	3,64	35	1	64
	7,5	15	50	0	36,2	24,2	60,4	3,774	20	0,5	79,5
9	9,1	15	100	0	36,4	33	69,4	3,279	0	0	100
	9,2	15	100	0	38,4	32,4	70,8	3,55	0	0	100
	9,3	15	100	0	37,2	30,3	67,5	3,732	0,25	0	99,75
	9,4	15	100	0	39,6	31,6	71,2	3,632	0,25	0	99,75
	9,5	15	100	0	37,7	31,3	69	3,826	0	0	100
11	11,1	15	200	0	36,4	34,5	70,9	3,724	1	1	98
	11,2	15	200	0	37,6	33,6	71,2	3,699	0	0	100
	11,3	15	200	0	36,6	33,1	69,7	3,697	0,5	0	99,5
	11,4	15	200	0	36,6	34	70,6	3,629	0	0	100
	11,5	15	200	0	36,7	33,5	70,2	3,465	1	0	99
13	13,1	25	50	0	32,6	18,2	50,8	3,843	15	3	82
	13,2	25	50	0	33,8	22,3	56,1	3,921	45	0	55
	13,3	25	50	0	36,8	14,9	51,7	3,504	50	0	50
	13,4	25	50	0	32,3	23,5	55,8	3,809	10	2,5	87,5
	13,5	25	50	0	31,7	18,1	49,8	3,947	45	0,5	54,5
15	15,1	25	100	0	24,1	10,2	34,3	3,837	0,5	1	98,5
	15,2	25	100	0	26,2	10,4	36,6	3,735	0,5	0	99,5
	15,3	25	100	0	25,7	10	35,7	3,887	0	1	99
	15,4	25	100	0	24,8	11,9	36,7	3,886	0	0,5	99,5
	15,5	25	100	0	23,8	8,8	32,6	3,829	0	0,5	99,5
17	17,1	25	200	0	25,4	6,5	31,9	3,464	1	0,5	98,5
	17,2	25	200	0	24	5,9	29,9	3,401	0	0	100
	17,3	25	200	0	24,4	6	30,4	3,478	0,5	0	99,5
	17,4	25	200	0	25,6	6,7	32,3	3,586	0	0	100
	17,5	25	200	0	24,3	5,2	29,5	3,614	0	0,5	99,5

Sample	Specimen	Distance	Speed	Surface status	Dispersive comp. [mJ/m²]	Polar comp. [mJ/m²]	Surface energy [mJ/m²]	Lap Shear testing-Peak load [kN]	Lap Shear testing %-adhesive failure	Lap Shear testing %-cohesive failure	Lap Shear testing %-paint failure
2	2,1	5	50	1	30,6	12,9	43,5	3,411	11,25	1,25	87,5
	2,2	5	50	1	29,3	12,2	41,5	3,49	0	0	100
	2,3	5	50	1	30,4	12,1	42,5	3,444	0,5	0	99,5
	2,4	5	50	1	31,9	17,9	49,8	3,403	20	0	80
	2,5	5	50	1	32,1	19	51,1	3,435	0	0	100
4	4,1	5	100	1	32,4	33,9	66,3	3,35	24,5	0,5	75
	4,2	5	100	1	32,1	33,3	65,4	3,504	37,5	0	62,5
	4,3	5	100	1	34,3	29,5	63,8	3,076	58,5	0,5	41
	4,4	5	100	1	34,6	29,7	64,3	3,235	32	0,5	67,5
	4,5	5	100	1	34,6	22,4	57	3,501	51,5	0,5	48
6	6,1	5	200	1	34,9	34,9	69,8	3,379	57,5	0	42,5
	6,2	5	200	1	34,3	34,4	68,7	2,632	80	0	20
	6,3	5	200	1	35,4	24,2	59,6	2,686	82,5	0	7,5
	6,4	5	200	1	35,5	23	58,5	3,235	40	0	60
	6,5	5	200	1	34,9	27,8	62,7	3,12	65	5	30
8	8,1	15	50	1	33,6	27,8	61,4	2,254	97,5	0	2,5
	8,2	15	50	1	34,3	27,7	62	2,02	96,25	3,75	0
	8,3	15	50	1	34,4	22,9	57,3	2,519	96	1	3
	8,4	15	50	1	33,3	28,8	62,1	1,819	92,5	0	7,5
	8,5	15	50	1	34,5	13,8	48,3	2,238	99	1	0
10	10,1	15	100	1	37,7	7,1	44,8	1,412	100	0	0
	10,2	15	100	1	35	15	50	1,364	100	0	0
	10,3	15	100	1	36,1	15,7	51,8	1,618	99	1	0
	10,4	15	100	1	38,5	18,3	56,8	1,562	100	0	0
	10,5	15	100	1	37,6	17,7	55,3	1,635	99,5	0,5	0
12	12,1	15	200	1	36,1	16,4	52,5	1,562	100	0	0
	12,2	15	200	1	37,8	17,3	55,1	1,994	95	5	0
	12,3	15	200	1	36,6	20,1	56,7	1,651	100	0	0
	12,4	15	200	1	38,3	20,5	58,8	2,016	97,5	2,5	0
	12,5	15	200	1	38,7	19,6	58,3	1,792	100	0	0
14	14,1	25	50	1	37,4	17,3	54,7	3,321	57,5	0	42,5
	14,2	25	50	1	37,9	12,9	50,8	1,683	100	0	0
	14,3	25	50	1	39,2	13	52,2	3,177	30	3	67
	14,4	25	50	1	38,5	13,8	52,3	3,334	25	1	74
	14,5	25	50	1	38,2	16,7	54,9	3,228	12,5	0	87,5
16	16,1	25	100	1	35,6	22,3	57,9	1,098	100	0	0
	16,2	25	100	1	35,4	22,4	57,8	1,36	100	0	0
	16,3	25	100	1	33,8	22,5	56,3	1,523	100	0	0
	16,4	25	100	1	32,3	16,3	48,6	1,498	100	0	0
	16,5	25	100	1	31,6	14	45,6	1,363	100	0	0
18	18,1	25	200	1	33,1	10,8	43,9	1,45	100	0	0
	18,2	25	200	1	32,5	12,5	45	1,562	100	0	0
	18,3	25	200	1	34,8	14,6	49,4	1,294	100	0	0
	18,4	25	200	1	32,3	10,9	43,2	0,995	100	0	0
	18,5	25	200	1	34,1	11,4	45,5	0,988	100	0	0

Sample	Specimen	Pre-treatment	Surface status	Dispersive comp. [mJ/m²]	Polar comp. [mJ/m²]	Surface energy [mJ/m²]	Lap Shear testing-Peak load [kN]	Lap Shear testing %-adhesive failure	Lap Shear testing %-cohesive failure	Lap Shear testing %-paint failure
20	20,1	none	1	28,1	12,2	40,3	0,679	100	0	0
	20,2	none	1	26,8	12,8	39,6	0,638	100	0	0
	20,3	none	1	26,9	17,6	44,5	0,583	100	0	0
	20,4	none	1	28,9	11,1	40	0,7	100	0	0
	20,5	none	1	27	16,7	43,7	0,777	100	0	0
21	21,1	solvent wiping	0	30,1	9,6	39,7	1,71	100	0	0
	21,2	solvent wiping	0	29,6	11,2	40,8	1,542	100	0	0
	21,3	solvent wiping	0	30,2	8,5	38,7	2,663	100	0	0
	21,4	solvent wiping	0	31,5	21	52,5	1,496	100	0	0
	21,5	solvent wiping	0	31,2	8,2	39,4	1,926	100	0	0
22	22,1	solvent wiping	1	35,3	18	53,3	0,413	100	0	0
	22,2	solvent wiping	1	35,6	18,8	54,4	0,528	100	0	0
	22,3	solvent wiping	1	35,3	18	53,3	0,454	100	0	0
	22,4	solvent wiping	1	35,6	20,7	56,3	0,492	100	0	0
	22,5	solvent wiping	1	35	21,9	56,9	0,255	100	0	0

Appendix III Response surface design

The following response surface design was created in the software Minitab 16.

AR-samples

Response Surface Regression: Peak load [kN] versus Distance; Speed

The analysis was done using coded units.

Estimated Regression Coefficients for Peak load [kN]

Term	Coef	SE Coef	T	P
Constant	3,67934	0,05233	70,304	0,000
Distance	0,18163	0,02633	6,898	0,000
Speed	-0,04860	0,02610	-1,862	0,070
Distance*Distance	-0,07993	0,04521	-1,768	0,085
Speed*Speed	-0,10905	0,05179	-2,106	0,042
Distance*Speed	-0,05731	0,03139	-1,826	0,076

S = 0,142953 PRESS = 1,04843
R-Sq = 63,58% R-Sq(pred) = 52,09% R-Sq(adj) = 58,91%

Analysis of Variance for Peak load [kN]

Source	DF	Seq SS	Adj SS	Adj MS	F	P
Regression	5	1,39119	1,39119	0,27824	13,62	0,000
Linear	2	1,16857	1,04320	0,52160	25,52	0,000
Distance	1	1,06032	0,97234	0,97234	47,58	0,000
Speed	1	0,10825	0,07086	0,07086	3,47	0,070
Square	2	0,15450	0,15450	0,07725	3,78	0,032
Distance*Distance	1	0,06389	0,06389	0,06389	3,13	0,085
Speed*Speed	1	0,09060	0,09060	0,09060	4,43	0,042
Interaction	1	0,06812	0,06812	0,06812	3,33	0,076
Distance*Speed	1	0,06812	0,06812	0,06812	3,33	0,076
Residual Error	39	0,79698	0,79698	0,02044		
Lack-of-Fit	3	0,17179	0,17179	0,05726	3,30	0,031
Pure Error	36	0,62519	0,62519	0,01737		
Total	44	2,18817				

Unusual Observations for Peak load [kN]

Obs	StdOrder	Peak load [kN]	Fit	SE Fit	Residual	St Resid	
21	21	3,279	3,683	0,048	-0,404	-3,00	R
33	33	3,504	3,778	0,055	-0,274	-2,08	R

R denotes an observation with a large standardized residual.

Estimated Regression Coefficients for Peak load [kN] using data in uncoded units

Term	Coef
Constant	2,86185
Distance	0,0516950
Speed	0,00534488
Distance*Distance	-7,99333E-04
Speed*Speed	-1,93867E-05
Distance*Speed	-7,64143E-05

SebumTEFO-samples

Response Surface Regression: Peak load [kN] versus Distance; Speed

The analysis was done using coded units.

Estimated Regression Coefficients for Peak load [kN]

Term	Coef	SE Coef	T	P
Constant	1,3866	0,14519	9,550	0,000
Distance	-0,7297	0,07305	-9,990	0,000
Speed	-0,4140	0,07241	-5,718	0,000
Distance*Distance	0,7288	0,12541	5,811	0,000
Speed*Speed	0,5653	0,14368	3,934	0,000
Distance*Speed	-0,2596	0,08708	-2,981	0,005

S = 0,396590 PRESS = 8,27041
R-Sq = 81,99% R-Sq(pred) = 75,71% R-Sq(adj) = 79,68%

Analysis of Variance for Peak load [kN]

Source	DF	Seq SS	Adj SS	Adj MS	F	P
Regression	5	27,917	27,917	5,5834	35,50	0,000
Linear	2	18,774	20,837	10,4187	66,24	0,000
Distance	1	14,738	15,696	15,6956	99,79	0,000
Speed	1	4,036	5,142	5,1419	32,69	0,000
Square	2	7,746	7,746	3,8728	24,62	0,000
Distance*Distance	1	5,311	5,311	5,3110	33,77	0,000
Speed*Speed	1	2,435	2,435	2,4346	15,48	0,000
Interaction	1	1,398	1,398	1,3980	8,89	0,005
Distance*Speed	1	1,398	1,398	1,3980	8,89	0,005
Residual Error	39	6,134	6,134	0,1573		
Lack-of-Fit	3	2,641	2,641	0,8802	9,07	0,000
Pure Error	36	3,494	3,494	0,0970		
Total	44	34,051				

Unusual Observations for Peak load [kN]

Obs	StdOrder	Peak load [kN]	Fit	SE Fit	Residual	St Resid
32	32	1,683	2,625	0,153	-0,942	-2,57 R

R denotes an observation with a large standardized residual.

Estimated Regression Coefficients for Peak load [kN] using data in uncoded units

Term	Coef
Constant	5,73212
Distance	-0,248335
Speed	-0,0254510
Distance*Distance	0,00728767
Speed*Speed	0,000100493
Distance*Speed	-3,46157E-04